Lateral flow assay modified with time-delay wax barriers as a sensitivity and signal enhancement strategy.

Amadeo Sena-Torralba [a]†, Duy Ba Ngo [b]†, Claudio Parolo [a], Liming Hu [a], Ruslan Álvarez [a], Jose Francisco Bergua [a], Giulio Rosati [a], Werasak Surareungchai [b d] and Arben Merkoçi [a c]*

a. Nanobioelectronics & Biosensors Group, Institut Català de Nanociència i Nanotecnologia (ICN2), CSIC and The Barcelona Institute of Science and Technology (BIST), Campus UAB, 08193, Bellaterra, Barcelona, Spain.
b. School of Bioresoures and Technology, King Mongkut's University of Technology Thonburi (KMUTT), Bangkok 10150, Thailand.
c. Catalan Institution for Research and Advanced Studies (ICREA), Pg. Lluís Companys 23, 08010 Barcelona, Spain.
d. Nanoscience and Nanotechnology Graduate Research Program, Faculty of Science, KMUTT, Bangkok 10140, Thailand

** arben.merkoci@icn2.cat*
† Amadeo Sena-Torralba and Duy Ba Ngo contributed equally to this work.

Keywords: Lateral flow, Sensitivity enhancement, Wax barrier, Point-of-Care, Optical biosensor

Abstract

The ease of use, low cost and quick operation of lateral flow assays (LFA) have made them some of the most common point of care biosensors in a variety of field. However, their generally low sensitivity has limited their use for more challenging applications, where the detection of low analytic concentrations is required. Here we propose the use of soluble wax barriers to selectively and temporarily accumulate the target and label nanoparticles on top of the test line (TL). This extended internal incubation step promotes the formation of the immune-complex, generating a 2.8-fold sensitivity enhancement and up to 96% signal enhancement compared to the conventional LFA for Human IgG (H-IgG) detection.

1. Introduction

During the last decade we have been observing an ever-growing need for fast and reliable sensing devices for healthcare, environmental and safety applications.(Turner, 2013, Malhotra et al., 2005) Both developed and developing countries are increasingly relying on the use of point of care tests (POCT) to keep up with the saturation of their health-care systems, to monitor the quality of their environmental resources and to prevent possible threats. The POCTs represent not only convenient analytical tools for rural regions (they

are cheap, portable and easy to use), but they are also establishing themselves as key monitoring devices in the busy centralized areas.(Price, 2001, Land et al., 2019, Chin et al., 2012) For example a faster diagnosis means faster therapy initiation and higher chances to control the spread of a disease; and it also means a quicker response time for starting a remediation campaign in a contaminated river. In this context LFAs are probably the most used POCT covering the widest variety of applications.(Quesada-González and Merkoçi, 2015, Posthuma-Trumpie et al., 2009) They serve as an excellent tool for healthcare,(Chen et al., 2016, Brangel et al., 2018) safety(Quesada-González et al., 2018, Mirasoli et al., 2012) and environmental applications(Hassan et al., 2019, Schubert-Ullrich et al., 2009, Raeisossadati et al., 2016).

Being fast and easy to use are key features for the POCTs, but they also come with the drawback that the sensitivity of the POCTs has no match with laboratory-based, slower, multi-steps sensing techniques. For example in the LFA the binding event between bio-receptors (antibodies, aptamers) and their targets happens in the order of seconds (the time required for the flow to pass the TL)(Gasperino et al., 2018, Miller et al., 2018), while in Enzyme-Linked Immunosorbent Assays (ELISA)(Van Weemen and Schuurs, 1971) incubation for several hours is common. Although for many applications the sensitivity of LFAs is sufficient, finding a way to improve it without affecting their being the POC would open a plethora of new applications. Here we are describing just that, a method to increase the time of the bio-recognition event, without affecting the ease of use and the overall sensing time of the LFAs.

The concept at the base of LFAs, is the use of capillary movement to guide the sample through different functional membranes.(Quesada-González and Merkoçi, 2015, Muhammad Sajid et al., 2015) Taking as example an immune-sandwich (non-competitive) assay, first the sample encounters the sample pad, where pre-stored biochemical reagents stabilizes its pH and ionic strength at their optimal values to maximize the signal to noise ratio.(Millipore, 2013) Then it flows to the conjugate pad, where the detection antibodies (generally labelled with coloured nanoparticles) recognize the target in the first bio-recognition event.(Quesada-González et al., 2019) Then the solution flows along the detection pad, where the complex target/labelled-antibody binds to the capture antibodies of the TL, during the second bio-recognition event. Finally the sample after passing through the control line (CL), reaches the

absorbent pad at the end of the LFA. Surprisingly most of the reported works trying to improve the sensitivity of LFA have focused on increasing the time for the first bio-recognition event, but depending on the flow-rate of the pads it can already take minutes. (Zhang et al., 2019, Tsai et al., 2018) Instead of the second bio-recognition event is always in the order of seconds, representing the real bottle neck for the sensitivity of the test.

The possibility to slow down or even temporarily stop the flow above the test line would increase the time for both bio-recognition events, boosting the sensitivity of the LFAs. Here we present how we achieved it by placing a soluble wax barrier 1 mm after the TL. Looking at previous works we find that wax structures were previously employed in LFAs just to control the flow (Giokas et al., 2014, Lai et al., 2019, Phillips et al., 2016, Rivas et al., 2014), but never to temporarily stop it. While some paper-based microfluidic devices did incorporate real barrier to achieve incubation steps, but they were introduced before the test line and were based on salt (He et al., 2019) or sugar(Lutz B, Liang T, Fu E, Ramachandran S, Kauffman P, 2013), which once dissolved can affect the ionic strength of the working buffer and thus the binding reaction. Instead, here, the wax barrier is printed on the surface of the nitrocellulose membrane and melted in order to assure its penetration through the membrane pores creating a hydrophobic barrier just after the TL, which is the place where the second bio-recognition event is taking place. The conjugate solution together with the sample solution flows along the nitrocellulose membrane towards the test line, giving time for the first binding event to occur. Once arrived to wax barrier, the solution stops temporarily on top of the test line until the barrier breaks due to the surfactant present on the strip (figure 1). In this sense, the thickness of the wax barrier and the concentration of surfactant can be carefully selected in order to modulate the incubation time and determine the ones that provide the highest sensitivity.

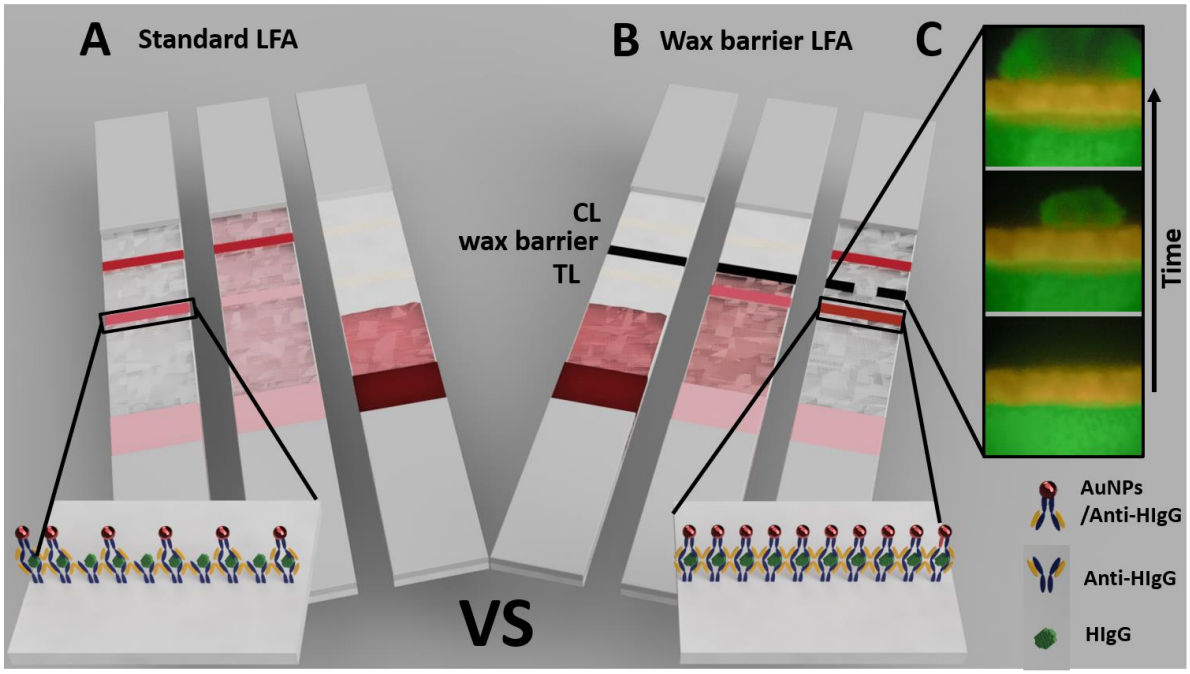

Figure 1. Schematic representation of the proposed strategy for the detection of H-IgG. (A) In the standard LFA the flow is constantly moving towards the absorbent pad and the bio-recognition event occurs within seconds. Few labelled antibodies are captured in TL, thus the signal intensity is weak. (B) In the LFA modified with a wax barrier, the flow is temporarily stopped on the TL. This increases the time for the bio-recognition event and boosts the assay's sensitivity. (C) Fluorescent microscope pictures (40X) of the wax barrier on the LFA strip. The wax barrier temporarily retains the solution. Once broken by the Tween-20, the solution goes through the barrier.

2. Experimental section

2.1. Materials and reagents

Goat anti-human IgG antibody, human IgG, bovine serum albumin (BSA), Tetrachloroauric acid (HAuCl4), trisodium citrate, phosphate buffer saline (PBS) tablets, sodium phosphate basic and dibasic, sodium tetraborate, boric acid sucrose and Tween 20 were purchased from Sigma Aldrich. Chicken anti-goat antibody was purchased from Abcam. Nitrocellulose membranes (CN95 and CN150) were purchased from Sartorius Stediem and CNPF200 from mdi. Cellulose membrane (CFSP001700) was purchased in Merck Millipore, glass fiber (Standard14) from GE Healthcare and supporting adhesive

cards were purchased from Kenosha. Decol food colorant red powder was purchased in Torten Deko and wax ink (Xerox 108R00935 black) was purchased in Xerox.

2.2. Instruments

Wax printer Xerox ColorQube 8580, Bioreagent dispenser (Imagene Technology), Microscope Olympus cellSense, Centrifuge Allegra 64R, Lateral flow strips cutter (Shanghai Kinbio Tech), Spectrophotometer SpectraMax ID3, SkanMulti (Skannex), TEM Technai F20.

2.3. Synthesis and characterization of gold nanoparticles

The gold nanoparticles (AuNPs) were synthesized following the Turkevich method(Turkevich et al., 1951) and were characterized with TEM (~ 15 nm) and spectrophotometer (absorbance peak at 515 nm) (figure S1 and S2), respectively. The AuNPs were adjusted to pH 9.2 using borate buffer (10 mM pH 9.2) and centrifuged at 14000 rpm for 30 minutes. Finally, they were re-suspended in 250 µL of PBS (10 mM, pH 7.4, 5% sucrose, 1% BSA and 0.5% tween-20) and dried in the glass fiber overnight. Moreover, the sample pad was blocked with PBS (10 mM, pH 7.4, 0.5% BSA and 0.05% to 0.1% tween-20) and dried overnight.

2.4. Conjugation of the AuNPs with anti H-IgG

The AuNPs were conjugated to antibodies against H-IgG following the procedure previously reported by our group.(Ambrosi et al., 2007) In order to check if the AuNPs were successfully conjugated with the antibodies, the absorbance spectrum was evaluated. As observed in figure S2, the maximum absorbance peak of the conjugated the AuNPs has a little red shift (about 5 nm), indicating the presence of the antibodies on the surface of the AuNPs.

3. Results and discussion

3.1. Evaluation of the retention time

When developing the POCT, reproducibility is one of the most important parameters to optimize. For this reason, we fixed the lateral flow strip dimensions to 6 x 0.3 cm and verified that the bed volume corresponds to 70 µL (figure S3). We then proceeded to optimize the barrier fabrication by printing black lines with different widths (0.01, 0.03,

0.05 y 0.1 mm) onto CN95 nitrocellulose membrane, and melting homogeneously the wax at 95 ° C for 5 minutes in the oven (figure S4). Next, we evaluated the time required for breaking the barriers at different concentrations of Tween-20, following the former optimized parameters. In particular, we fabricated lateral flow strips containing different concentrations of Tween-20 (0.05%, 0.1%, 0.5% and 0.1%) in the sample pad and the AuNPs in the conjugate pad. The retention time was measured from the moment at which the AuNPs reached the wax barrier until they crossed the barrier.

As a result, we generated a matrix providing the wax barrier width and Tween-20 concentration that provide different retention times (Table 1 and figure S5). As expected, the retention time increases increasing barrier width and decreasing Tween-20 concentration. In particular, we achieved the longest retention time (12 minutes) by employing barriers of 0.05 mm and a concentration of Tween-20 of 0.1%; while the shortest retention time (1 minute) required a barrier width of 0.01 mm and 0.5% Tween-20. Width of 0.1 mm and Tween-20 concentration of 0.05%, showed to be not suitable for the assay as the barriers broke once the AuNPs solution was already dried out.

Moreover, we printed the barriers in a slower flow rate nitrocellulose membrane (CNPF200 mdi), in order to evaluate how the use of smaller pore sizes can affect the retention time. In this case, the pressure applied by the wax printing process compacted the pore of the nitrocellulose, thereby the flow could not even reach the TL.

Table 1. Retention times on CN95 with different wax barrier width and %Tween-20

Wax width (mm)	0.5% Tween-20	0.1% Tween-20	0.05% Tween-20
0.01	1.40 ± 0.42 min	3.93 ± 1.55 min	NB
0.03	2.25 ± 0.13 min	7.64 ± 1.19 min	NB
0.05	7.23 ± 0.86 min	11.45 ± 1.33 min	NB
0.10	NB	NB	NB

* NB: No Breaking, which means that the solution dried out before breaking the wax barrier.

3.2. Evaluation of the sensitivity enhancement in LFA

Finally, after determining the optimum conditions to achieve the longest flow retention, we performed the lateral flow immunoassay for H-IgG detection. In order to check if there is a correlation between the retention time on the TL and the sensitivity enhancement,

we fabricated the strips without barriers and with barriers width of 0.01, 0.03 and 0.05 mm. In this regard, we used CN95 and 0.1% Tween-20 as surfactant to break the barriers. We were expecting to see a progressive sensitivity enhancement when using higher width barriers, obtaining the highest sensitivity by using 0.05 mm width barrier, since this is the one that provides the longest retention time. Next, we prepared the strips by fixing anti H-IgG antibodies (1 mg mL^{-1}) in the TL and anti-goat antibodies (1 mg mL^{-1}) in the CL, both in 10 mM PB buffer pH 7.4. Moreover, we conjugated the AuNPs with anti H-IgG by following the procedure previously reported by our group,(Ambrosi et al., 2007) explained in the experimental section. Furthermore, we performed calibration curves using serial dilutions of H-IgG (0 ng mL^{-1} to 10^3 ng mL^{-1}). Finally, we evaluated the signal intensity in both the TL and CL the by taking a picture of the strips using a LFA scanner and analyzing them with Image J software.(Schneider et al., 2012) We took the pictures of the strips once the AuNPs solution had completely reached the absorbent pad. Eventually, we used the signal values of the TL and the CL after background signal subtraction, and normalized the signal value by dividing TL over CL.

Figure S6 shows the calibration curves obtained when using CN95 and CN150 without the barriers and CN95 with 0.01, 0.03 and 0.05 mm width barriers. As observed the normalized optical density increases upon the detection of higher concentrations of H-IgG. Figure S7 shows the pictures of the lateral flow strips after performing the assays. In order to evaluate the sensitivities obtained with each condition we performed a linear fitting from 10 to 1000 ng mL^{-1} and we considered the slope values (figure 2A). As we were expecting, a higher sensitivity is achieved when using wider barriers, as this assures a longer interaction time between the antibodies in TL, AuNPs and the analyte. The highest sensitivity is achieved when using a 0.05 mm width barrier, which provides a 2.8-fold enhancement compared to the same nitrocellulose without barriers. It is noteworthy that, conversely to the reported, there isn't an outstanding sensitivity improvement when reducing the flow rate by using a smaller pore nitrocellulose membrane, as in the case of CN150. (Millipore, 2013, NanoComposix, 2016) Besides, we have proved that the outstanding sensitivity enhancement is obtained only when temporarily stopping the flow above the TL.

Moreover, we calculated the limit of detection (LoD) and quantification (LoQ) achieved for every tested condition. The LoD was calculated as $Optical\ density_{LOD} = blank + 3\ \sigma_{blank}$ (i.e. the corresponding value of blank sample plus 3 times its standard deviation). (Armbruster and Pry, 2008) The LoD for CN95, CN150 and CN95 with 0.01, 0.03 and 0.05 mm width barriers were 35.01, 73.23, 21.67, 18.71, 14.47 ng·mL^{-1}, respectively. Furthermore, the LoQ, calculated as $Optical\ density_{LOD} = blank + 10\ \sigma_{blank}$, were 2129.09, 1909.76, 1164.38, 87.49, 41.19 ng·mL^{-1}, respectively. We obtained the lowest LoD and LoQ values by setting the barriers at the condition that permitted the highest retention time of the conjugate solution on the TL.

In figure 2B, we show pictures of the LFA strips after performing the calibration curve assay from 10 to 1000 ng mL^{-1} using CN95, CN150 non-modified with the wax barriers and CN95 modified with 0.01, 0.03 and 0.05 mm width barriers. As observed, there is a signal enhancement in TL when introducing the wax barriers in to the system. The percentage signal enhancement was calculated taking as reference the normalized optical density of the strips with CN95 and without the wax barriers (Table S2). As observed, the percentage signal increase is higher for increasing concentrations of H-IgG. The highest percentage signal increase is 96%, and was achieved for 1000 ng mL^{-1} when using CN95 with a 0.05 mm width barrier.

Finally, we proved that a longer incubation time of the conjugate solution over the TL didn't favor the generation of non-specific signal in TL. As shown in figure S7, the signal in TL for blank samples (0 ng mL^{-1} of H-IgG) is not higher when using wider wax barriers, as we obtained the highest TL signal for the blank sample when using the CN150 nitrocellulose membrane.

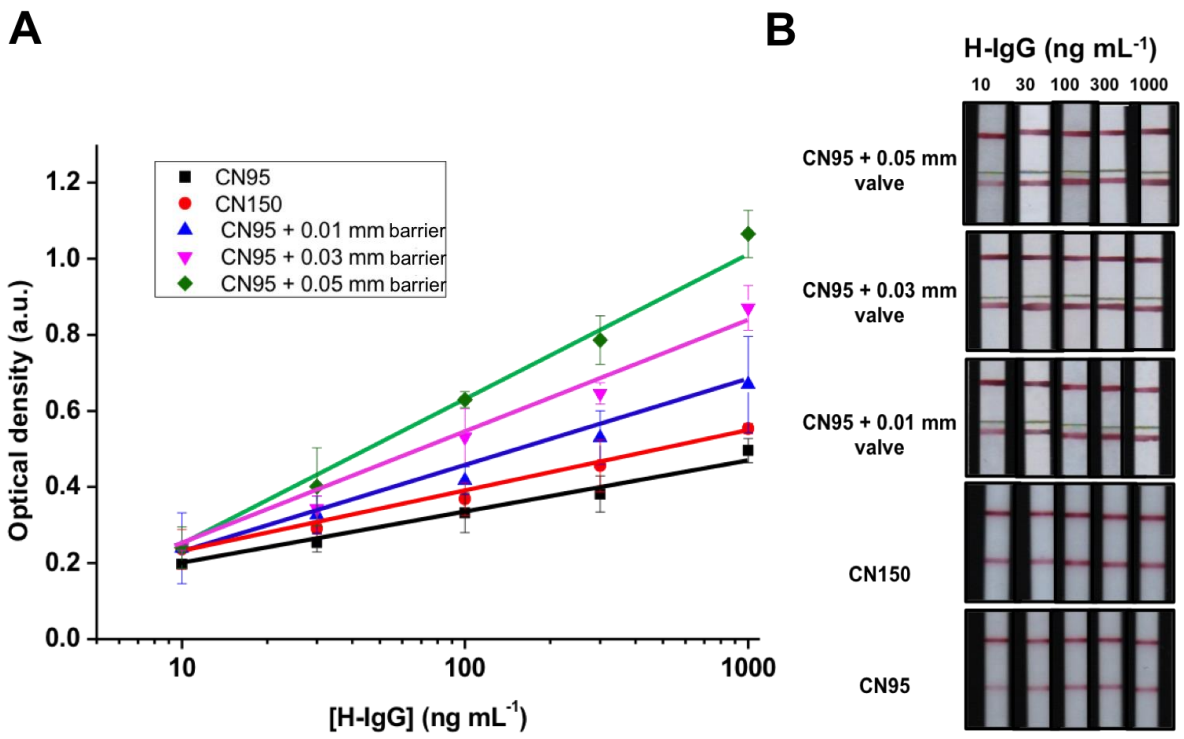

Figure 2. The LFA for H-IgG detection using time-delay barriers. **(A)** Calibration curve from 10 to 1000 ng mL^{-1} showing the optical density linear range when using CN95 (Optical density = 0.0631 ln [H-IgG (ng mL^{-1})] + 0.0433 r^2=0.98) and CN150 non-modified with the wax barriers (Optical density = 0.0695 ln [H-IgG (ng mL^{-1})] + 0.0627 r^2=0.99) and CN95 modified with 0.01 (Optical density = 0.0925 ln [H-IgG (ng mL^{-1})] + 0.0124 r^2=0.99), 0.03 (Optical density = 0.1359 ln [H-IgG (ng mL^{-1})] - 0.1165 r^2=0.96) and 0.05 mm width barriers (Optical density = 0.1767 ln [H-IgG (ng mL^{-1})] - 0.2056 r^2=0.98). **(B)** Pictures of the LFA strips after performing the calibration curve assay from 10 to 1000 ng mL^{-1} using CN95, CN150 non-modified with the wax barriers and CN95 modified with 0.01, 0.03 and 0.05 mm width barriers.

4. Conclusion

In conclusion, we have developed a LFA modified with time-delay barriers as a strategy for sensitivity and signal enhancement. We have achieved an inner incubation time of 12 minutes, which produced a 2.8-fold enhancement in sensitivity and up to 96% signal enhancement. We believe the proposed method represents an outstanding solution to

improve the analytical performance of LFAs, without sacrificing their ease-of-use and low cost.

Acknowledgments

We acknowledge financial support from NACANCELL project PCIN-2016-066 (program Euronanomed 2). This work is also funded by the CERCA Program/Generalitat de Catalunya. The ICN2 is funded by the CERCA programme / Generalitat de Catalunya. ICN2 acknowledges the support of the Spanish MINECO for the Project MAT2017-87202-P and through the Severo Ochoa Centers of Excellence Program under Grant SEV2201320295. Amadeo Sena-Torralba acknowledge Autonomous University of Barcelona (UAB) for the possibility of performing this work inside the framework of Biotechnology Ph.D. Programme. Duy Ba Ngo gratefully acknowledges Petchra Pra Jom Klao Doctoral, King Mongkut's University of Technology Thonburi (KMUTT) in Thailand and Sensor Technology, School of Bioresources and Technology, KMUTT, Thailand.

References

Ambrosi, A., Castañeda, M.T., Killard, A.J., Smyth, M.R., Alegret, S., Merkoçi, A., 2007. Double-codified gold nanolabels for enhanced immunoanalysis. Anal. Chem. 79, 5232–5240.

Armbruster, D.A., Pry, T., 2008. Limit of blank, limit of detection and limit of quantitation. Clin. Biochem. Rev. 29 Suppl 1, S49–52.

Brangel, P., Sobarzo, A., Parolo, C., Miller, B.S., Howes, P.D., Gelkop, S., Lutwama, J.J., Dye, J.M., McKendry, R.A., Lobel, L., Stevens, M.M., 2018. A Serological Point-of-Care Test for the Detection of IgG Antibodies against Ebola Virus in Human Survivors. ACS Nano 12, 63–73. https://doi.org/10.1021/acsnano.7b07021

Chen, Y., Sun, J., Xianyu, Y., Yin, B., Niu, Y., Wang, S., Cao, F., Zhang, X., Wang, Y., Jiang, X., 2016. A dual-readout chemiluminescent-gold lateral flow test for multiplex and ultrasensitive detection of disease biomarkers in real samples. Nanoscale 8, 15205–15212. https://doi.org/10.1039/c6nr04017a

Chin, C.D., Linder, V., Sia, S.K., 2012. Commercialization of microfluidic point-of-care diagnostic devices. Lab Chip 12, 2118–2134. https://doi.org/10.1039/c2lc21204h

Gasperino, D., Baughman, T., Hsieh, H. V., Bell, D., Weigl, B.H., 2018. Improving Lateral Flow Assay Performance Using Computational Modeling. Annu. Rev. Anal. Chem. 11, 219–244. https://doi.org/10.1146/annurev-anchem-061417-125737

Giokas, D.L., Tsogas, G.Z., Vlessidis, A.G., 2014. Programming fluid transport in paper-based microfluidic devices using razor-crafted open channels. Anal. Chem. 86, 6202–6207. https://doi.org/10.1021/ac501273v

Hassan, A.H.A., Bergua, J.F., Morales-Narváez, E., Mekoçi, A., 2019. Validity of a single antibody-based lateral flow immunoassay depending on graphene oxide for highly sensitive determination of E. coli O157:H7 in minced beef and river water. Food Chem. 297, 124965. https://doi.org/10.1016/j.foodchem.2019.124965

He, X., Liu, Z., Yang, Y., Li, L., Wang, L., Li, A., Qu, Z., Xu, F., 2019. Sensitivity Enhancement of Nucleic Acid Lateral Flow Assays through a Physical-Chemical Coupling Method: Dissoluble Saline Barriers. ACS Sensors 4, 1691–1700. https://doi.org/10.1021/acssensors.9b00594

Lai, Y., Tsai, C., Hsu, J., Lu, Y., 2019. Microfluidic Time-Delay Valve Mechanism on Paper-Based Devices for Automated Competitive ELISA. Micromachines 10, 837.

Land, K.J., Boeras, D.I., Chen, X.S., Ramsay, A.R., Peeling, R.W., 2019. REASSURED diagnostics to inform disease control strategies, strengthen health systems and improve patient outcomes. Nat. Microbiol. 4, 46–54. https://doi.org/10.1038/s41564-018-0295-3

Lutz B, Liang T, Fu E, Ramachandran S, Kauffman P, Y.P., 2013. Dissolvable fluidic time delays for programming multi-step assays in instrument-free paper diagnostics. Lab Chip 13, 2840–7. https://doi.org/10.1038/jid.2014.371

Miller, B.S., Parolo, C., Turbé, V., Keane, C.E., Gray, E.R., McKendry, R.A., 2018. Quantifying Biomolecular Binding Constants using Video Paper Analytical Devices. Chem. - A Eur. J. 24, 9783–9787. https://doi.org/10.1002/chem.201802394

Millipore, M., 2013. Rapid Lateral Flow Test Strips Considerations for Product Development.

Mirasoli, M., Buragina, A., Dolci, L.S., Guardigli, M., Simoni, P., Montoya, A., Maiolini, E., Girotti, S., Roda, A., 2012. Development of a chemiluminescence-based quantitative lateral flow immunoassay for on-field detection of 2,4,6-trinitrotoluene. Anal. Chim.

319 Acta 721, 167–172. https://doi.org/10.1016/j.aca.2012.01.036
320 Muhammad Sajid, Abdel-Nasser Kawde, Muhammad Daud, 2015. Designs, formats and
321 applications of lateral flow assay: A literature review. J. Saudi Chem. Soc. 19, 689–
322 705. https://doi.org/10.1016/J.JSCS.2014.09.001
323 NanoComposix, 2016. Lateral flow assay development guide. nanoComposix Lateral
324 Flow Handb. v.1.4.
325 Phillips, E.A., Shen, R., Zhao, S., Linnes, J.C., 2016. Thermally actuated wax valves for
326 paper-fluidic diagnostics. Lab Chip 16, 4230–4236.
327 https://doi.org/10.1039/c6lc00945j
328 Posthuma-Trumpie, G.A., Korf, J., Van Amerongen, A., 2009. Lateral flow (immuno)assay:
329 Its strengths, weaknesses, opportunities and threats. A literature survey. Anal.
330 Bioanal. Chem. 393, 569–582. https://doi.org/10.1007/s00216-008-2287-2
331 Price, C.P., 2001. Regular review: Point of care testing. Br. Med. J. 322, 1285–1288.
332 https://doi.org/10.1136/bmj.322.7297.1285
333 Quesada-González, D., Jairo, G.A., Blake, R.C., Blake, D.A., Merkoçi, A., 2018. Uranium (VI)
334 detection in groundwater using a gold nanoparticle/paper-based lateral flow
335 device. Sci. Rep. 8, 8–15. https://doi.org/10.1038/s41598-018-34610-5
336 Quesada-González, D., Merkoçi, A., 2015. Nanoparticle-based lateral flow biosensors.
337 Biosens. Bioelectron. 73, 47–63. https://doi.org/10.1016/j.bios.2015.05.050
338 Quesada-González, D., Sena-Torralba, A., Wicaksono, W.P., de la Escosura-Muñiz, A.,
339 Ivandini, T.A., Merkoçi, A., 2019. Iridium oxide (IV) nanoparticle-based lateral flow
340 immunoassay. Biosens. Bioelectron. 132, 132–135.
341 https://doi.org/10.1016/j.bios.2019.02.049
342 Raeisossadati, M.J., Danesh, N.M., Borna, F., Gholamzad, M., Ramezani, M., Abnous, K.,
343 Taghdisi, S.M., 2016. Lateral flow based immunobiosensors for detection of food
344 contaminants. Biosens. Bioelectron. 86, 235–246.
345 https://doi.org/10.1016/j.bios.2016.06.061
346 Rivas, L., Medina-Sánchez, M., de la Escosura-Muñiz, A., Merkoçi, A., 2014. Improving
347 sensitivity of gold nanoparticle-based lateral flow assays by using wax-printed
348 pillars as delay barriers of microfluidics. Lab Chip 14, 4406–4414.
349 https://doi.org/10.1039/c4lc00972j
350 Schneider, C.A., Rasband, W.S., Eliceiri, K.W., 2012. NIH Image to ImageJ: 25 years of
351 image analysis. Nat. Methods 9, 671–675. https://doi.org/10.1038/nmeth.2089

Schubert-Ullrich, P., Rudolf, J., Ansari, P., Galler, B., Führer, M., Molinelli, A., Baumgartner, S., 2009. Commercialized rapid immunoanalytical tests for determination of allergenic food proteins: An overview. Anal. Bioanal. Chem. 395, 69–81. https://doi.org/10.1007/s00216-009-2715-y

Tsai, T.T., Huang, T.H., Chen, C.A., Ho, N.Y.J., Chou, Y.J., Chen, C.F., 2018. Development a stacking pad design for enhancing the sensitivity of lateral flow immunoassay. Sci. Rep. 8, 1–10. https://doi.org/10.1038/s41598-018-35694-9

Turkevich, J., Stevenson, P.C., Hillier, J., 1951. A study of the nucleation and growth processes in the synthesis of colloidal gold. Discuss. Faraday Soc. 11, 55–75.

Turner, A.P.F., 2013. Biosensors: Sense and sensibility. Chem. Soc. Rev. 42, 3184–3196. https://doi.org/10.1039/c3cs35528d

Van Weemen, B.K., Schuurs, A.H.W.M., 1971. Immunoassay using antigen-enzyme conjugates. FEBS Lett. 15, 232–236. https://doi.org/10.1016/0014-5793(71)80319-8

Zhang, S.F., Liu, L.N., Tang, R.H., Liu, Z., He, X.C., Qu, Z.G., Li, F., 2019. Sensitivity enhancement of lateral flow assay by embedding cotton threads in paper. Cellulose 26, 8087–8099. https://doi.org/10.1007/s10570-019-02677-6

Supplementary Material

Supplementary material can be found at:

https://www.journals.elsevier.com/biosensors-and-bioelectronics/XXXX